

Hemagglutinin-Neuraminidase-Independent Fusion Activity of Simian Virus 5 Fusion (F) Protein: Difference in Conformation between Fusogenic and Nonfusogenic F Proteins on the Cell Surface

MASATO TSURUDOME,^{1*} MORIHIRO ITO,¹ MACHIKO NISHIO,¹ MITSUO KAWANO,¹
HIROSHI KOMADA,² AND YASUHIKO ITO¹

*Department of Microbiology, Mie University School of Medicine, Tsu, Mie 514-8507,¹ and
Department of Microbiology, Suzuka University of Medical Science and Technology,
Suzuka, Mie 510-0226,² Japan*

Received 27 November 2000/Accepted 26 June 2001

The fusion (F) protein of simian virus 5 (SV5) strain W3A is known to induce cell fusion in the absence of hemagglutinin-neuraminidase (HN) protein. In contrast, the F protein of SV5 strain WR induces cell fusion only when coexpressed with the HN protein, the same as do other paramyxovirus F proteins. When Leu-22 in the subunit F2 of the WR F protein is replaced with the counterpart (Pro) in the W3A F protein, the resulting mutant L22P induces extensive cell fusion by itself. In the present study, we obtained anti-L22P monoclonal antibodies (MAbs) 21-1 and 6-7, whose epitopes were located in the middle (amino acids [aa] 227 to 320) of subunit F1. The amino-terminal region (aa 20 to 47) of subunit F2 was also involved in the formation of MAb 21-1 epitope. Flow cytometric analysis revealed that both the MAbs reacted very faintly with native WR F protein that was expressed on the cell surface whereas they reacted efficiently with native L22P irrespective of whether it is cleaved into F1 and F2. However, by heating the cells at 47°C after mild formaldehyde fixation, the epitopes for MAb 6-7 and mAb 21-1 in the WR F protein were exposed and the reactivity of the MAbs with the WR F protein became comparable to their reactivity with L22P. Thus, the two MAbs seem to distinguish the difference in native conformation between fusogenic mutant L22P and its parental nonfusogenic WR F protein. The native conformation of L22P may represent an intermediate between native and postfusion conformations of a typical paramyxovirus F protein.

The subfamily *Paramyxovirinae* of the family *Paramyxoviridae* contains three genera, *Respirovirus*, *Rubulavirus*, and *Morbillivirus* (9, 31, 40). Two kinds of glycoproteins, hemagglutinin-neuraminidase (HN) and fusion (F) protein, are inserted in the viral envelope of the members of the genera *Respirovirus* and *Rubulavirus*. The HN protein is responsible for binding to sialic acid-containing cellular molecules and for enzymatic cleavage of the sialoconjugate, while the F protein is involved in envelope-to-cell and cell-to-cell fusion (cell fusion) (9, 31).

The F protein is activated from a precursor (F0) when cleaved by cellular protease(s) and forms a disulfide-bonded subunit structure consisting of F1 and F2, which is a prerequisite for the fusion process (22, 42). The well-conserved hydrophobic domain (fusion peptide) at the amino terminus of F1 is exposed by the cleavage (25, 29) and is considered likely to be directly involved in the fusion event (17, 37). The cleavage also results in a conformational change of the F protein (13, 25, 29, 54). Three heptad repeat (HR) domains are found in the F1 ectodomain (6, 18). The HR1 domain is immediately next to the carboxyl terminus of the fusion peptide, while the HR2 domain is close to the transmembrane domain. The HR3 domain is located between the FR1 and HR2 domains (18) and is followed by a highly conserved stretch of eight cysteine

residues (the cysteine-rich domain) (6). Crystallographic analyses have shown that polypeptide fragments representing the HR1 domain of the F protein of simian virus 5 (SV5) or human respiratory syncytial virus can form a trimeric coiled-coil structure, to which three antiparallel helices of the polypeptide fragments representing the HR2 domain can bind (1, 33, 60). On the other hand, an electron microscopic study of purified human respiratory syncytial virus F protein has indicated that the lollipop-shaped rod observed in the purified F protein possibly represents the “postfusion” conformation and harbors the antiparallel trimeric coiled-coil structure in the stem region (5), which is consistent with the conclusion drawn from the crystallographic study (60). The antiparallel trimeric coiled-coil structures of the F proteins are similar to the core structures reported for Ebola virus GP2 (56), human immunodeficiency virus gp41 (7, 57), and simian immunodeficiency virus gp41 (4). Since all the antiparallel trimeric coiled-coil structures found in the above viral proteins resemble to the core structure of influenza virus HA2 in postfusion conformation that is formed at low pH (3), they may represent the final and most stable core structures of the proteins, which are formed either during or after membrane fusion. However, the native structures of these proteins, except for HA2, have not definitely been clarified as yet, leaving a possibility that their antiparallel coiled-coil structures are already present in their native state, as supposed by Caffrey et al. (4). Importantly, in this context, there is evidence indicating that the antiparallel

* Corresponding author. Mailing address: Department of Microbiology, Mie University School of Medicine, 2-174 Edobashi, Tsu, Mie 514-8507, Japan. Phone and fax: (81) 59-231-5008. E-mail: turudome@doc.medic.mie-u.ac.jp.

trimeric coiled-coil structure is not present in the uncleaved precursor of SV5 F protein (13).

Although the F protein seems to play a pivotal role in the fusion event, the fusion-promoting function of the HN protein is considered indispensable for most of the F proteins (2, 15, 16, 21, 26, 34, 36, 41, 47, 51). In support of this idea, it has been demonstrated that homotypic HN and F proteins are physically associated with each other in the virus-infected cells or in the plasmid-transfected cells (11, 44, 58). Furthermore, analyses using chimeric proteins have indicated that the HN-F interaction may take place between the stalk region of the HN protein (10, 12, 46, 51) and the middle region (including the HR3 domain and part of the cysteine-rich domain) of F1 (50). However, the mechanism by which the HN protein promotes the fusing function of the F protein and triggers the conformational change of the F protein is still unclear.

As the first step in solving this problem and elucidating the molecular basis of the fusion process of paramyxoviruses, it seems necessary to clarify precise structural aspects of the F protein before it undergoes conformational changes that lead to fusion. In this context, the requirement of the HN protein for fusion is a disadvantage of the paramyxovirus F proteins. It is therefore important to note the exceptional fact that the F protein of SV5 strain W3A mediates cell fusion in the absence of the HN protein (24, 38). By using a plasmid expression system in BHK cells, we have confirmed that the W3A F protein exhibits a remarkable fusing activity when expressed alone (27). In contrast, the F protein of another SV5 strain, WR, required coexpression of the HN protein (WR HN protein or mumps virus [MuV] HN protein) to induce cell fusion. By mutational analysis of the three amino acids that were not conserved between the F proteins of the W3A and WR viruses, a critical amino acid (Pro-22) was identified in the W3A F2 (27). Accordingly, a mutant F protein L22P in which a leucine residue at position 22 of the WR F protein was replaced with proline induced cell fusion when expressed alone. However, it is not known how Pro-22 contributes to the HN-independent fusion activity, and there are at least two possibilities. One possibility is that Pro-22 is directly involved in the interaction of the F protein with its putative receptor on the target membrane, which triggers the conformational change in the F protein, leading to fusion. The other possibility is that the presence of Pro-22 somehow destabilizes the F protein so that it can easily undergo a conformational change on contact with the target membrane or on docking with the putative receptor as suggested (30). If the latter is the case, there could be some difference in the native conformation between L22P and its parental WR F protein, which has Leu-22 instead.

In the present study, we prepared monoclonal antibodies directed against L22P and used them to probe differences between L22P and the WR F protein. Consequently, the antibodies revealed a striking difference in conformation between the native structures of L22P and the WR F protein on the cell surface.

MATERIALS AND METHODS

Cells. Human cervical carcinoma-derived HeLa cells, mouse L929 cells, and baby hamster kidney-derived BHK cells were maintained in Eagle's minimum essential medium (MEM) supplemented with 5% calf serum.

Rabbit antisera. Antipeptide rabbit serum, α -5F2, specific for the carboxyl-terminal sequence (KLLQPIGENLETIRNQLIPT) of the WR F2 subunit, was prepared by Sawady Technology (Tokyo, Japan) as described previously (28). Anti-SV5 rabbit serum was purchased from Denka Institute of Biological Science (Niigata, Japan).

Recombinant plasmids. As described previously (27, 51), the cDNA encoding the WR F protein, L22P, the SV41 F protein, or SV41 HN was cloned in the plasmid expression vector pcDL-SR α 296 (SR α), in which the gene expression is under control of the SV40 early promoter and/or R-U5 sequence of the human T-cell leukemia virus type 1 long terminal repeat. The SR α plasmid was a generous gift from Yutaka Takebe (National Institute of Infectious Diseases, Tokyo, Japan). The recombinant SR α plasmid encoding MuV HN (47) was kindly donated by Akio Yamada and Kiyoshi Tanabayashi (National Institute of Infectious Diseases).

To create chimeric recombinant plasmids, six restriction sites (*Hind*III, *Bbe*I, *Hind*III, *Sac*II, *Spl*I, and *Vsp*I) were introduced into both or either of the recombinant SR α plasmids encoding L22P or SV41 F protein by site-directed mutagenesis as described below. The chimeric structures of the resulting recombinant plasmids were confirmed by direct nucleotide sequencing using an ABI PRISM 310 genetic analyzer (Applied Biosystems Division, Perkin-Elmer, Foster City, Calif.).

Site-directed mutagenesis. Introduction of mutation-generating synthetic oligonucleotides into the target recombinant plasmid was performed by using the U.S.E. Mutagenesis Kit (Amersham Pharmacia Biotech AB, Uppsala, Sweden) as specified by the manufacturer, as described previously (28, 50).

Transient expression of F proteins. Cells were seeded at 5×10^5 cells/well in six-well culture plates (Costar, Cambridge, Mass.) and incubated at 37°C for 24 h in MEM supplemented with 10% fetal calf serum. Each recombinant plasmid (2 or 4 μ g/well) was then added to the cells by the calcium phosphate method (20). After 2 h of incubation at 37°C, the cells were treated with 15% glycerol in HEPES-buffered saline (50 mM HEPES, 0.75 mM sodium phosphate, 140 mM NaCl) at room temperature (RT) for 3 min, and incubated in MEM plus 10% fetal calf serum (FCS) for 24 h unless otherwise specified.

Establishment of an L929 cell line stably expressing L22P. Subconfluent L929 cells grown in a 100-mm dish was cotransfected with plasmid pKan2 (5 μ g) and the recombinant plasmid (20 μ g) encoding L22P by using Lipofectin (GIBCO BRL, Grand Island, N.Y.) as specified by the manufacturer. After incubation at 37°C for 8 h, the medium was replaced with MEM containing 10% calf serum. Then, after incubation for 2 days, the cells were suspended in MEM containing 10% FCS, 1 mg of Geneticin (GIBCO BRL) per ml, and 0.2% agarose and were cultured in the soft agar for 3 weeks. Expression of the F protein on the cells was detected by immunofluorescence microscopy (described below) with anti-SV5 antiserum after fixation with 3.7% formaldehyde. Plasmid pKan2, which contains the G418 (Geneticin) resistance gene and promoters identical to those of SR α , was kindly provided by Yutaka Takebe. An L929 cell line expressing L22P was established and designated L-L22P.

MAbs. To obtain hybridoma cell lines producing anti-L22P monoclonal antibodies (MAbs), a C3H/He mouse was immunized with the L-L22P cells. Prior to immunization, the L-L22P cells were treated with 50 μ g of mitomycin C (Sigma Aldrich, St. Louis, Mo.) per ml in phosphate-buffered saline (pH 7.4) (PBS) at 37°C for 3 h and washed with MEM. Spleen cells of the immunized mouse were fused with SP2/O-Ag14 myeloma cells as described previously (53). Culture fluids of the resulting hybridoma cells were screened by using 3.7% formaldehyde-fixed L-L22P cells and L929 cells (as a negative control) in enzyme-linked immunosorbent assay and in indirect immunofluorescence microscopy (described below). Consequently, 16 hybridoma clones that produced anti-L22P MAbs were obtained, of which we used two representative clones, MAb 6-7 (isotype immunoglobulin G2a [IgG2a]) and MAb 21-1 (IgG2a), in the present study. MAb 108S1 (IgG2a), which is specific for human parainfluenza virus type 2 HN (52), was used as the isotype-matched control. The MAb specific for the human lysosomal protein Lamp-1 was from American Research Products (Belmont, Mass.) and was of the IgG1 isotype. The MAb specific for SV41 F (MAb 31A-2) was reported previously (49).

Indirect-immunofluorescence microscopy. HeLa cells cultured on glass coverslips in six-well culture plates were transfected with 2 μ g of recombinant plasmid per well. After incubation at 37°C for 24 h, the cells were fixed with 3.7 or 0.37% formaldehyde in PBS at RT for 1 h and washed three times with PBS. In some experiments, the fixed cells were permeabilized with 0.1% Triton X-100 in PBS at RT for 1 h. For immunofluorescent staining, the fixed cells were treated successively with MAbs (undiluted culture fluids of hybridoma cells) at RT for 1 h and fluorescein isothiocyanate (FITC)-conjugated goat anti-mouse immunoglobulins (diluted 1:100 with PBS) (Cappel, Cochranville, Pa.) at RT for 1 h. Otherwise, the cells were treated successively with anti-F2 peptide rabbit serum

(α -5F2, diluted 1:100 with PBS) and FITC-conjugated goat anti-rabbit immunoglobulins (1:800) (Cappel). The results were observed by using a fluorescence microscope (Olympus, Tokyo, Japan).

Flow cytometry. The amount of F proteins on the cell surface was measured by flow cytometric analysis as described previously (28, 45). Briefly, HeLa cells grown in six-well culture plates were transfected with 4 μ g of recombinant plasmid encoding each F protein per well. After 24 h of incubation at 37°C, the cells were suspended in 0.02% EDTA in PBS. They were then immunostained either with MAbs (undiluted culture fluid) and FITC-conjugated goat anti-mouse immunoglobulins (1:100) or with anti-SV5 rabbit serum (1:100) and FITC-conjugated goat anti-rabbit immunoglobulins (1:800). The mean fluorescence intensity (MFI) of 2×10^4 cells was measured on a FACScan instrument (Becton Dickinson). For each antibody, the MFI given by the cells transfected with F protein-encoding plasmid was expressed after subtracting that given by the control cells transfected with SR α plasmid. In some experiments, prior to immunostaining, the cell suspensions were fixed with 0.37 or 3.7% formaldehyde and washed with PBS. Aliquots of the 0.37% formaldehyde-fixed cells in PBS were heated at 47°C for 5 min in a water bath.

Confocal laser microscopy. HeLa cells grown on coverslips in a six-well culture plate were transfected with 2 μ g of plasmid encoding WR F protein per well, fixed with 3.7% formaldehyde at 24 h posttransfection, and permeabilized with 0.1% Triton X-100. The cells were then successively treated with MAb 21-1 (IgG2a), FITC-conjugated rat anti-mouse IgG2a (Zymed Laboratories, San Francisco, Calif.), anti-Lamp-1 MAb (IgG1), and tetramethylrhodamine-5-iso-thiocyanate (TRITC)-conjugated goat anti-mouse IgG1 (Southern Biotechnology Associates, Birmingham, Ala). The results were observed by using a confocal laser microscope (Carl Zeiss, Jena, Germany).

Denaturation of the F protein on the cell surface. HeLa cells grown on coverslips were transfected with the WR F-encoding plasmid (2 μ g/well), and after incubation for 24 h the cells were fixed with 0.37% formaldehyde in PBS (pH 7.4) at RT for 1 h. Heat denaturation (ranging from 37 to 70°C) of the fixed cells was carried out for 5 min by putting the coverslips into PBS in a glass beaker placed in a water bath. To obtain temperatures from 80 to 120°C, the coverslips were put into PBS in a glass dish and autoclaved at the indicated temperatures for 5 min. Chemical denaturation of the fixed cells with methanol or urea (6 M urea, 85 mM HEPES-NaOH, 85 mM KCl, 58 mM MgCl₂ [pH 7.4]) was performed at RT for 30 min. The fixed cells were treated with cathepsin (5 or 50 nM) at 28°C for 6 h by using cathepsin G (Elastin Products, Owensville, Mo.) or cathepsin H (Calbiochem, La Jolla, Calif.) in potassium phosphate buffer (pH 5.0) supplemented with 2.5 mM EDTA and 2.5 mM dithiothreitol. Acid treatment of unfixed cells was performed by using 50 mM citrate-buffered saline (pH 5.0 to 7.4) at 37°C for 30 min, and the cells were then fixed with 3.7% formaldehyde. After each denaturing treatment, the cells were subjected to indirect immunofluorescence microscopy as described above without permeabilization with Triton X-100.

Radioimmunoprecipitation. HeLa cells grown in six-well culture plates were transfected with recombinant plasmid (4 μ g/well), incubated at 37°C for 20 h in MEM containing 10% FCS, and washed once with methionine- and cystine-depleted Dulbecco's modified MEM (DMEM) (GIBCO BRL). After incubation in the fresh methionine- and cystine-depleted DMEM for 1 h, the cells were labeled with 500 μ Ci of Pro-mix L-[³⁵S] in vitro cell-labeling mix (Amersham Pharmacia Biotech Japan, Tokyo, Japan) per ml in the methionine- and cystine-depleted DMEM for 3 h, washed with chilled PBS, and lysed on ice for 15 min with lysis buffer (1% Triton X-100, 137 mM NaCl, 3 mM β -glycerophosphate, 3 mM EDTA, 1 mM phenylmethylsulfonyl fluoride, 25 mM HEPES [pH 7.6]). The cell lysates were clarified by centrifugation (13,000 \times g for 5 min), and the radiolabeled proteins in the cell lysates were immunoprecipitated by anti-SV5 rabbit serum (diluted 1:20 with PBS) or MAbs (undiluted culture fluids of hybridoma cells) and analyzed by sodium dodecyl sulfate-polyacrylamide gel electrophoresis (SDS-PAGE) as described previously (52). In some experiments, the transfected cells were labeled for 30 min and chased in chase medium (MEM supplemented with 5% calf serum, 5 mM methionine, and 5 mM cysteine) for 2 h in the presence or absence of 5 μ g of acetylated trypsin per ml.

RESULTS

Fusion activity of L22P in different cell lines. We have previously reported that the mutant L22P was able to induce HN-independent cell fusion in BHK cells while its parental WR F protein was not (27). L22P was also capable of inducing cell fusion in HeLa cells but not in L929 cells (data not shown).

However, in L929 cells, L22P was expressed inefficiently and induced very weak cell fusion even when coexpressed with mumps virus (MuV) HN protein (data not shown). Therefore, we could not fully exclude the possibility that the apparent resistance of L929 cells to the fusion activity of L22P was simply due to the low expression level. Nonetheless, this observation led us to establish an L929 cell line, L-L22P, which stably expressed L22P. The L-L22P cells were free of syncytial cells, whereas L22P was efficiently expressed on the cell surface and cleaved into F1 and F2 (data not shown). Interestingly, prominent cell fusion could be induced when the cells were transfected with MuV HN-encoding plasmid or cocultivated with BHK cells (data not shown). Therefore, the L22P on the L-L22P cell surface was biologically active and able to undergo conformational changes that lead to cell fusion when triggered by coexpressed HN or by a putative host cell factor (s) on the cocultured BHK cell membrane. However, it is still an open question why L22P does not mediate cell fusion by itself in L929 cells.

Difference in antigenicity between L22P and WR F protein on the cell surface. By immunizing a C3H/He mouse with the L-L22P cells, we obtained 16 hybridoma clones which secreted MAbs directed against L22P. As shown in Fig. 1A, the representative MAbs, 6-7 and 21-1, similarly immunoprecipitated L22P, which was recombinantly expressed and cleaved into F1 and F2 in HeLa cells. Accordingly, flow cytometric analysis demonstrated that MAbs 6-7 and 21-1 were equally reactive with native L22P expressed on the HeLa cell surface (Table 1). However, both the MAbs were poorly reactive with surface-localized native WR F protein, whose expression level was comparable to that of L22P as measured by anti-SV5 rabbit serum. These observations indicate that there is a difference in antigenicity between the native L22P and WR F protein on the cell surface. The low reactivity of the MAbs with the WR F protein could be explained by the single amino acid difference at position 22 between the WR F protein and L22P. However, it seemed unlikely that the epitopes for the MAbs were not present in the WR F protein, since both MAbs had the ability to immunoprecipitate detergent-solubilized WR F protein (data not shown). Together, these observations led us to hypothesize that the epitopes for the MAbs are cryptic in the surface-localized native WR F protein.

Difference in antigenicity between L22P and the WR F protein is independent of cleavage. As described above, L22P was able to induce cell fusion in HeLa cells by itself. Therefore, to analyze possible differences in native conformation between the fusogenic mutant L22P and its parental nonfusogenic WR F protein, it seemed necessary to compare the conformations of the F proteins before cleavage activation. Thus, we created mutant F proteins, Se-L22P and Se-WRF, so that the cleavage site of L22P and the WR F protein should be replaced with that of Sendai virus F protein (Fig. 1C). Sendai virus F protein is known to remain uncleaved in most culture cells unless treated with trypsin (22, 23). Accordingly, neither of the mutants was cleaved in HeLa cells in the absence of exogenously added acetylated trypsin (Fig. 1B). Furthermore, Se-L22P was able to mediate extensive cell fusion in HeLa cells by itself only when treated with acetylated trypsin, while Se-WRF was not (data not shown). As shown in Fig. 1B, MAb 6-7 could immunoprecipitate Se-WRF as efficiently as it immunoprecipitated

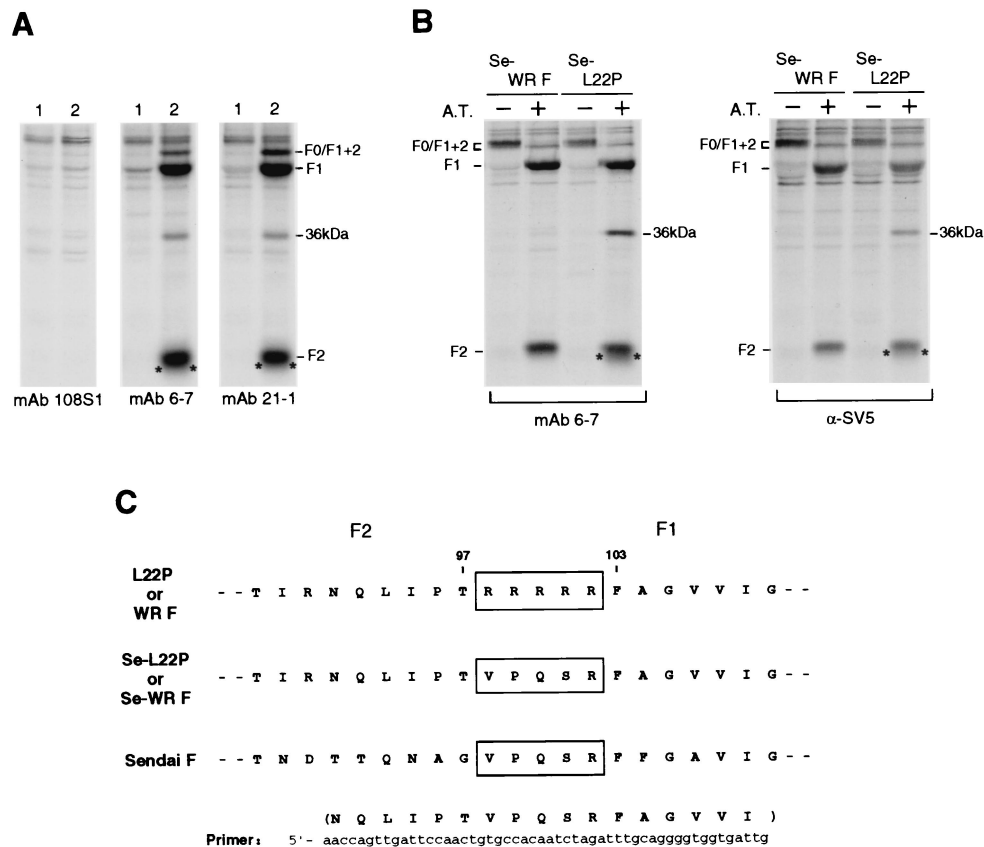


FIG. 1. (A) Immunoprecipitation of L22P from the lysates of transfected HeLa cells. HeLa cells grown in a six-well culture plate were transfected with 4 μ g of SR α plasmid (lane 1) or the recombinant plasmid encoding L22P (lane 2) per ml, incubated for 20 h, starved for 1 h in methionine- and cystine-depleted DMEM, and labeled with 500 μ Ci of Pro-mix L-[35 S] in vitro cell-labeling mix per ml for 3 h. The cells were then lysed with the lysis buffer as described in Materials and Methods. Aliquots of the cell lysates were subjected to immunoprecipitation with MAb 6-7 or 21-1, and the precipitates were analyzed by SDS-PAGE (13% polyacrylamide) under reducing conditions. MAb 108S1 is the isotype-matched negative control that is specific for parainfluenza virus type 2 HN. The 36-kDa band is an unidentified protein that was coprecipitated with L22P either by MAb 6-7 or by MAb 21-1. Asterisks indicate uncharacterized populations that migrate slightly faster than does L22P subunit F2. (B) Immunoprecipitation of Se-L22P and Se-WRF transiently expressed in HeLa cells. Cells grown in a six-well culture plate were transfected with 4 μ g of recombinant plasmid encoding Se-L22P or Se-WRF per well. After 21 h of incubation, the cells were starved for 1 h in methionine- and cystine-depleted DMEM. Then the cells were labeled with 500 μ Ci of Pro-mix L-[35 S] in vitro cell-labeling mix per ml for 30 min and chased for 2 h in the presence (+) or absence (-) of 5 μ g of acetylated trypsin (A.T.) per ml. The cell lysates were subjected to immunoprecipitation with MAb 6-7 or anti-SV5 rabbit serum, and the precipitates were analyzed by SDS-PAGE (13% polyacrylamide gel) under reducing conditions. The 36-kDa band is an unidentified protein that was coprecipitated with Se-L22P by MAb 6-7 or by anti-SV5 rabbit serum from the cell extract that was prepared after treatment with acetylated trypsin. Asterisks indicate uncharacterized populations that migrate slightly faster than does Se-L22P subunit F2. (C) Strategy for construction of the mutants Se-L22P and Se-WRF. Se-L22P and Se-WRF were created by site-directed mutagenesis so that the cleavage site preceding F1 was replaced with the counterpart of Sendai virus (Fushimi strain) F protein (GenBank accession number D00152). The cleavage site (five arginine residues) in the parent L22P or WR F proteins, and the corresponding sequences in the mutants and Sendai virus F protein are boxed.

Se-L22P, indicating that the MAb epitope was present in both the mutant F proteins. Intriguingly, MAb 6-7 seemed to immunoprecipitate the cleaved form of Se-WRF or Se-L22P more efficiently than it immunoprecipitated the uncleaved form, while anti-SV5 serum did not clearly show this tendency. On the other hand, in the presence of acetylated trypsin, unidentified proteins of 36 kDa and those that migrated slightly faster than F2 were coprecipitated with Se-L22P either by MAb 6-7 or by anti-SV5 rabbit serum but were not coprecipitated with Se-WRF (Fig. 1B). These unidentified proteins were also coprecipitated with L22P (Fig. 1A) but not with the WR F protein (data not shown). Therefore, Pro-22 in L22P or in Se-L22P seemed to be involved in the appearance of these

unidentified proteins. Further characterization of these proteins is under way in our laboratory.

These results demonstrate that Se-L22P and Se-WRF are not cleaved unless they are treated with acetylated trypsin and that MAb 6-7 can immunoprecipitate either of the proteins. Then, flow cytometric analysis of Se-L22P and Se-WRF was performed, in which the F protein-expressing cells were not treated with acetylated trypsin. As shown in Table 1, MAbs 6-7 and 21-1 only poorly recognized Se-WRF on the cell surface, while they reacted with Se-L22P even more efficiently than with L22P. These observations indicate that the epitopes for MAbs 6-7 and 21-1 are cryptic in the native WR F protein on the cell surface irrespective of whether it is cleaved into F1 and

TABLE 1. Antigenicity of surface-localized F proteins^a

Antibody	Mean fluorescence intensity			
	L22P	WR F	Se-L22P	Se-WRF
MAb 21-1	279	10	464	15
MAB 6-7	286	53	518	56
α -SV5	444	329	347	271

^a Prior to immunostaining and flow cytometry, transfected HeLa cells were suspended in EDTA-PBS. For each antibody, the mean fluorescence intensity of 2×10^4 cells which were transfected with F protein-encoding recombinant plasmid, was expressed after subtracting that of control cells transfected with SR α plasmid.

F2. It also seems important to note that the epitopes for MAbs 6-7 and 21-1 are already exposed on L22P before cleavage activation.

Effect of formaldehyde fixation on the MAB epitopes. Next, to further investigate the antigenic difference between the WR F protein and L22P, we performed immunofluorescence microscopy by using unfixed HeLa cell monolayers. Briefly, after 24 h of transfection, HeLa cell monolayers on glass coverslips were treated with the MAbs. The cells were then fixed with 3.7% formaldehyde and treated with FITC-conjugated secondary antibody. The results indicated that MAbs 6-7 and 21-1 immunostained surface-localized WR F protein only faintly or not at all, respectively, while they clearly immunostained surface-localized L22P (data not shown). These observations are fairly consistent with the data obtained from flow cytometry (Table 1). To our surprise, however, when the transfected HeLa cell monolayers were first fixed with 3.7% formaldehyde and then treated with antibodies, MAB 6-7 clearly immunostained surface-localized WR F protein while MAB 21-1 failed to do so (data not shown). Therefore, this observation was quantitatively confirmed by flow cytometry in which the cells were fixed with 3.7% formaldehyde before being immunostained (Table 2): the reactivity of MAB 6-7 with the WR F protein became considerably elevated (MFI, 389) while that of MAB 21-1 increased only marginally (MFI, 43). It was also revealed that the reactivity of both MAbs with L22P also increased significantly after fixation with 3.7% formaldehyde.

These results suggest that the MAB 6-7 epitope, which is cryptic in the surface-localized native WR F protein, can be exposed to some extent by denaturation with 3.7% formaldehyde.

The MAB 21-1 epitope in the WR F protein is exposed in the lysosome. On the other hand, the MAB 21-1 epitope in the surface-localized WR F protein could not be detected even when the cells were fixed with 3.7% formaldehyde as described above. However, when the WR F-expressing HeLa cell monolayers were permeabilized after 3.7% formaldehyde fixation and then immunostained with MAB 21-1, weak but significant fluorescence was observed at the perinuclear region by fluorescence microscopy (data not shown). The WR F molecules, which were detected at the perinuclear region by MAB 21-1, were shown to colocalize with the lysosomal membrane protein Lamp-1 by confocal laser microscopy (data not shown). Since there is evidence showing that SV5 F protein does not undergo clathrin-mediated endocytosis in infected CV-1 cells (32), we assume that the recombinantly expressed WR F protein is sorted to the lysosome either from the cell surface by bulk-

TABLE 2. Antigenicity of surface-localized F proteins after denaturation^a

Antibody	Mean fluorescence intensity					
	3.7% F		0.37% F		0.37% F + 47°C	
	L22P	WR F	L22P	WR F	L22P	WR F
MAB 21-1	1,231	43	487	0	1,194	974
MAB 6-7	1,383	389	410	0	1,133	1,111
α -SV5	1,293	973	297	220	370	565

^a Prior to immunostaining and flow cytometry, transfected HeLa cells were suspended with EDTA-PBS and fixed with 3.7% formaldehyde (3.7% F) or with 0.37% formaldehyde (0.37% F). Aliquots of the 0.37% formaldehyde-fixed cells were heated at 47°C for 5 min in PBS (3.7% F + 47°C). For each antibody, the mean fluorescence intensity of 2×10^4 cells, which were transfected with the F protein-encoding recombinant plasmid, was expressed after subtracting that of control cells transfected with SR α plasmid.

phase endocytosis or from the *trans*-Golgi network during transportation process. In any case, the MAB 21-1 epitope is exposed in the lysosome, whereas it is cryptic in the surface-localized WR F protein regardless of fixation.

Effect of denaturation on the antigenicity of the WR F protein. As described so far, MAB 21-1 did not react with the surface-localized WR F molecules but recognized those in the lysosome, indicating that the MAB 21-1 epitope in the WR F protein may be exposed as a result of degradation in the lysosome. Therefore, several attempts to mimic the environment in the lysosome were made in order to expose the MAB 21-1 epitope that might be cryptic in the surface-localized WR F protein. First, HeLa cells expressing the WR F protein were treated with acid (pH 5.0 to 6.0), but this treatment did not expose the MAB 21-1 epitope (data not shown). Second, the WR F-expressing cells were mildly fixed with 0.37% formaldehyde and treated with the lysosomal proteases (cathepsin G or H) at pH 5.0, but these procedures again did not expose the MAB 21-1 epitope (data not shown). As shown in Fig. 2, when the WR F-expressing HeLa cells were mildly fixed with 0.37% formaldehyde and not permeabilized, MAB 21-1 did not show even faint fluorescence, consistent with the data from flow cytometry (Table 2). Third, the WR F-expressing cells, were denatured by chemical treatment with urea or methanol after fixation with 0.37% formaldehyde, but neither treatment exposed the MAB 21-1 epitope in the surface-localized WR F protein (Fig. 2). Lastly, when the WR F-expressing cells were heated at 47°C for 5 min after fixation with 0.37% formaldehyde, the MAB 21-1 epitope was clearly exposed on the surface-localized WR F protein (Fig. 2).

Therefore, this observation was certified quantitatively by flow cytometric analysis (Table 2). The reactivity of MAbs 21-1 and 6-7 with the WR F protein increased very significantly when the 0.37% formaldehyde-fixed cells were heated at 47°C for 5 min, while it was undetectable when the cells were merely fixed with 0.37% formaldehyde. The reactivity of MAbs with L22P was also elevated by heating the 0.37% formaldehyde-fixed cells, but the level did not exceed that when the cells were fixed with 3.7% formaldehyde. Intriguingly, the reactivity of anti-SV5 antiserum with the WR F protein was more strongly elevated by heating than was the reactivity with L22P.

These results thus indicate that when the F proteins are heated at 47°C after 0.37% formaldehyde fixation, the reactivi-

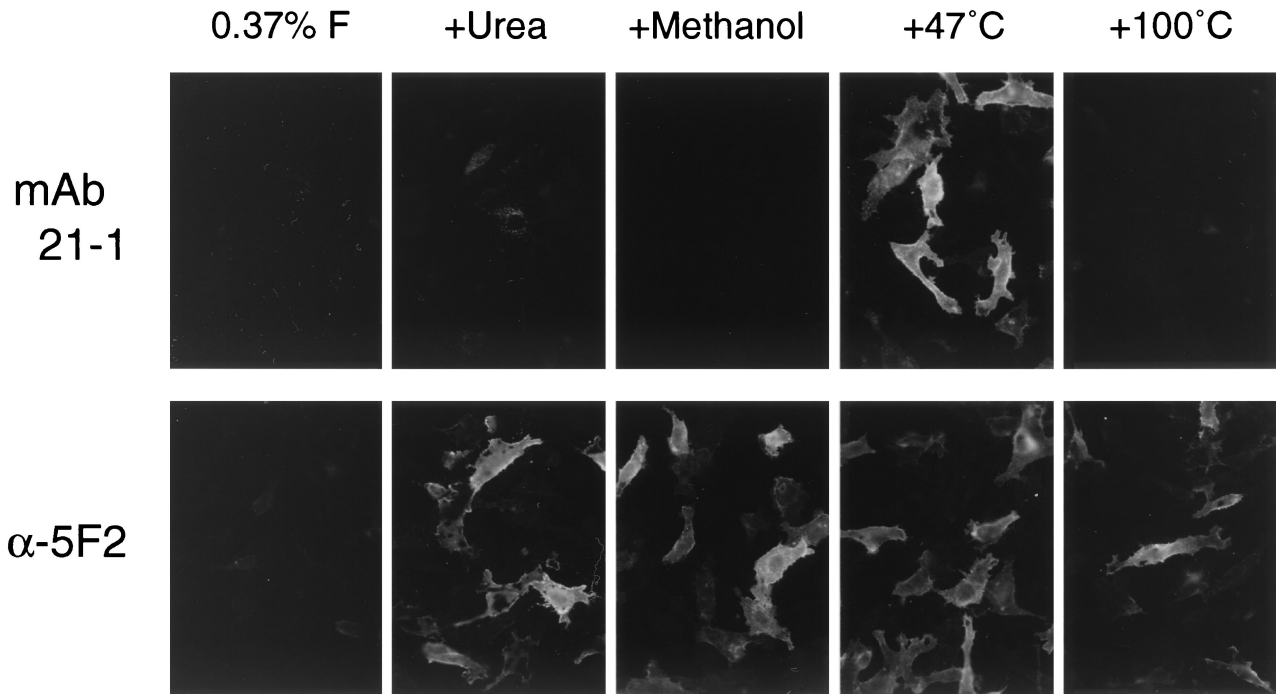


FIG. 2. Fluorescence microscopic analysis of the effects of various denaturing treatments on the WR F protein. HeLa cells grown on coverslips in a six-well culture plate were transfected with 2 μ g of plasmid encoding WR F protein per well. The cells were fixed with 0.37% formaldehyde in PBS (0.37% F) at 24 h posttransfection but were not permeabilized. The formaldehyde-fixed cells were then treated at RT for 30 min with 6 M urea or methanol. Otherwise, the fixed cells were heated at 47 or 100°C for 5 min in PBS. Finally, the treated cells were immunostained with MAb 21-1 or anti-F2 peptide rabbit serum (α -5F2), followed by FITC-conjugated secondary antibodies as described in Materials and Methods. Magnification, \times 135.

ity of MAbs 6-7 and 21-1 with the WR F protein becomes indistinguishable from their reactivity with L22P. It should be pointed out that the MAb 21-1 epitope was also clearly exposed when the WR F protein-expressing cells were heated at 47°C without formaldehyde fixation but was not exposed efficiently when the cells were fixed with 3.7% formaldehyde before being heated (data not shown). The MAb 21-1 epitope in the WR F protein was also exposed when the 0.37% formaldehyde-fixed cells were heated at 50, 70, or 90°C but was not exposed at 37 or 42°C (data not shown). Importantly, the MAb 21-1 epitope in the WR F protein was undetectable when the 0.37% formaldehyde-fixed cells were heated at 100°C (Fig. 2). On the other hand, the epitope for α -5F2 rabbit serum was also cryptic in the surface-localized WR F protein when the cells were fixed with 0.37% formaldehyde, but it could be exposed either by the chemical treatments or by heating at 47°C (Fig. 2). The epitope for α -5F2 antiserum was also detectable even when heated at 100°C (Fig. 2) or 120°C (data not shown), in accordance with the reactivity of the antiserum with the WR F protein in the Western blot (28).

These results suggest that heating the cells at 47°C after 0.37% formaldehyde fixation mediates a conformational change in the WR F protein, resulting in maximal exposure of the epitopes for MAbs 21-1 and 6-7.

Epitope mapping for MAbs. As described so far, the epitopes for MAbs 21-1 and 6-7 were exposed on the surface-localized native L22P but not maximally. By contrast, both the epitopes were cryptic in the surface-localized native WR F protein. However, both the epitopes in the WR F protein

became exposed as efficiently as those in L22P after heating at 47°C after 0.37% formaldehyde fixation. Furthermore, MAbs 6-7 and 21-1 were not able to recognize L22P or the WR F protein in the Western blot (data not shown) whereas the MAbs immunoprecipitated those that were solubilized with detergent. Therefore, it could be strongly suggested that the epitopes were conformation dependent and that Pro-22 at the amino terminus of L22P F2 was not simply the constituent. Therefore, to map the MAb epitopes on L22P, chimeric analyses were carried out by immunofluorescence microscopy, and the results obtained from eight chimeric proteins between L22P and SV41 F protein are summarized in Fig. 3 (representative immunofluorescent staining data are shown in Fig. 4.) As anticipated, the chimeric protein L22P-A, in which residues 1 to 47 (harboring the Pro-22) were derived from L22P and the remainder were derived from SV41 F protein, was not recognized by MAb 21-1 or by MAb 6-7. Instead, this chimera was recognized by the anti-SV41 F MAb, 31A-2 (Fig. 3). On the other hand, MAb 21-1 reacted faintly with L22P-CDEFG (also shown in Fig. 4) and L22P-DEFG, suggesting that blocks D to G on the L22P F1 partly contained the MAb 21-1 epitope. The reactivity of MAb 21-1 with these chimeras, L22P-CDEFG and L22P-DEFG, could not be enhanced by heating at 47°C after fixation with 0.37% formaldehyde (data not shown). Interestingly, when we combined the L22P-derived blocks A and D to G, the resulting chimera, L22P-ADEFG, was clearly recognized by MAb 21-1 (Fig. 3). Among blocks D to G, only block D was indispensable for the MAb 21-1 epitope, since the MAb reacted with L22P-ADE, L22P-ADFG, and L22P-AD but did

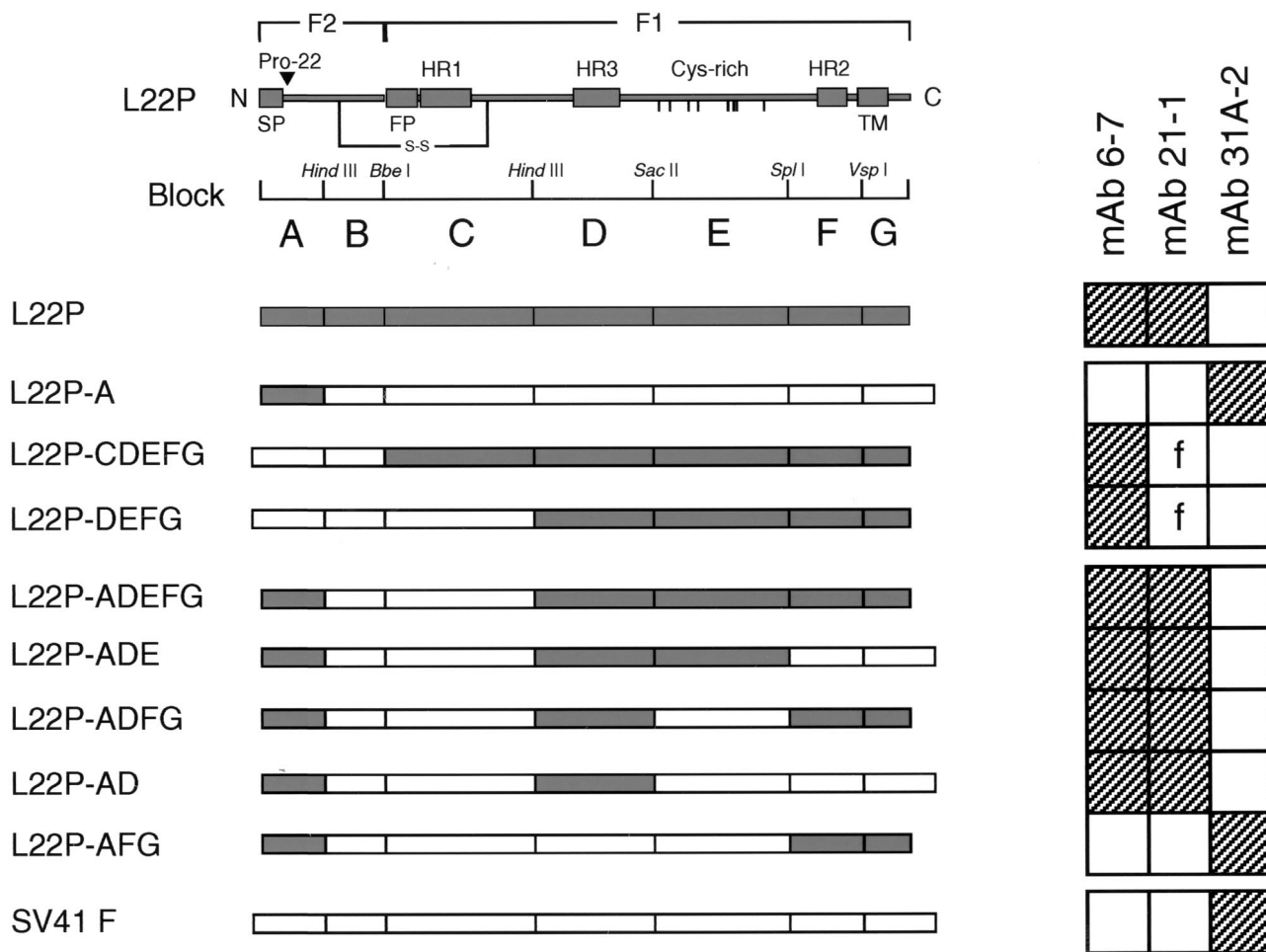


FIG. 3. Epitope mapping of MABs by using chimeric F proteins between L22P and SV41 F protein. At the top of the figure is a schematic of L22P in which the characteristic domains are indicated (SP, signal peptide; FP, fusion peptide; HR, heptad repeat domain; Cys-rich, cysteine-rich domain; TM, transmembrane domain). To create chimeric proteins, L22P was theoretically divided into seven blocks (designated A to G) according to the characteristic domains and restriction sites were introduced into the cDNAs encoding L22P and/or SV41 F protein in accordance with the division. Presented below the schematic is the diagram of the resulting chimeric F proteins between L22P and SV41 F protein. The name of a given chimeric protein reflects the blocks derived from L22P. For example, L22P-A has L22P-derived block A (a solid box) and the rest (corresponding to blocks B to G) from SV41 F protein (open boxes). Presented on the right is the summary of the reactivity of MABs with the chimeric and the parental F proteins as judged by indirect immunofluorescence microscopy (examples are shown in Fig. 4). Hatched squares represent positive staining, while open squares indicate negative staining. The letter f in the two open squares indicates a faint staining pattern (shown in Fig. 4).

not react with L22P-AFG (Fig. 3). Thus, as represented by the chimera L22P-AD, a given chimeric protein that had two L22P-derived blocks, A (amino acids [aa] 1 to 47) and D (aa 227 to 320), were definitely recognized by MAb 21-1. Since the signal peptide (aa 1 to 19) at the F2 amino terminus should be absent from the mature L22P, the amino acids within the amino terminus (aa 20 to 47) of F2 and those within the middle (aa 227 to 320) of F1 seemed necessary to form the MAb 21-1 epitope. On the other hand, the epitope for MAb 6-7 was mapped to the amino acids in the middle of F1 (aa 227 to 320), because MAb 6-7 recognized the chimera L22P-DEFG as well as L22P-AD (Fig. 3).

It seemed of interest that the chimera L22P-CDEFG, which had SV41 F-derived F2 and L22P-derived F1 (Fig. 3), induced syncytium formation in HeLa cells in the absence of HN (data not shown), suggesting that the HN-independent fusion activ-

ity of L22P was intrinsically carried by the F1 subunit. Of the remaining seven chimeric proteins, only one (L22P-AFG) showed HN-dependent fusion activity, in which it induced cell fusion in HeLa cells when coexpressed with SV41 HN or with MuV HN but not with SV5 (W3A) HN (data not shown).

DISCUSSION

Our present study has shown that the epitopes for MABs 6-7 and 21-1 are cryptic in the cell surface-localized native WR F protein. By contrast, they are exposed on the surface-localized native L22P. Importantly, both the epitopes are also exposed on the Se-L22P mutant, an uncleaved form of L22P, which does not induce cell fusion unless it is cleaved by acetylated trypsin. Therefore, the epitopes for MABs 6-7 and 21-1 seem readily exposed on the surface-localized L22P before under-

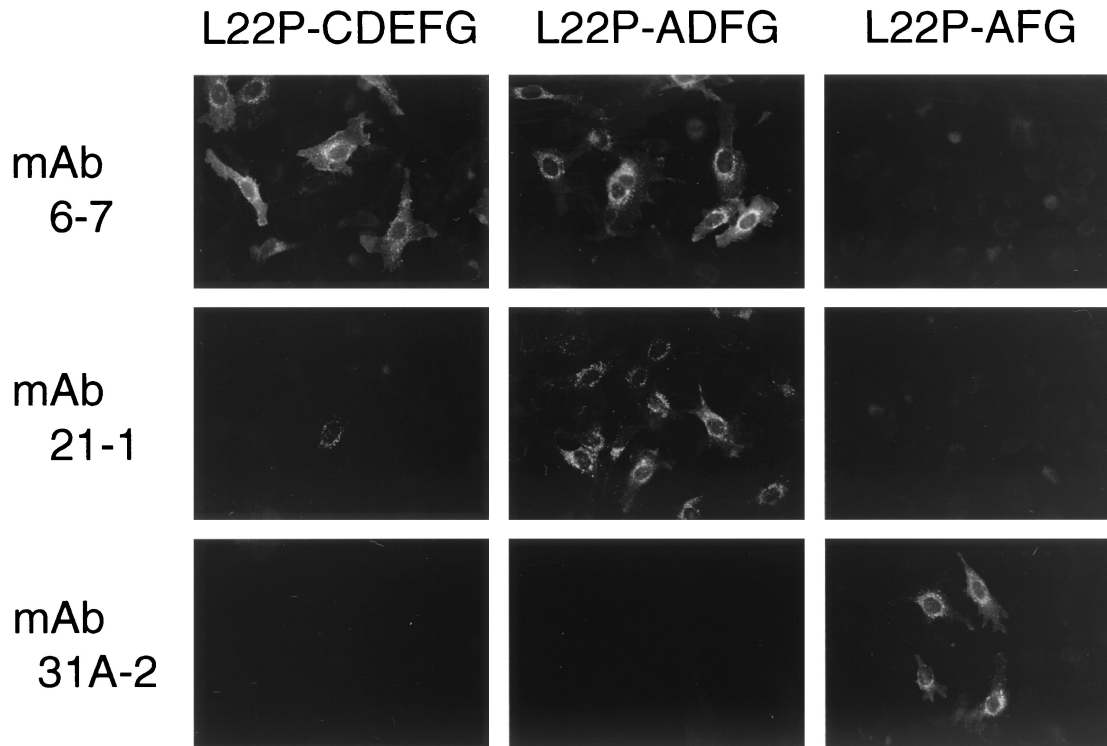


FIG. 4. Indirect immunofluorescence microscopy of chimeric F proteins. Representative staining patterns are shown. HeLa cells grown on coverslips in a six-well culture plate were transfected with 2 μ g of plasmid encoding either the chimeric F protein or SV41 F protein per well. The cells were fixed with 3.7% formaldehyde at 24 h posttransfection and permeabilized with 0.1% Triton X-100. Then they were immunostained with MAbs followed by FITC-conjugated secondary antibody as described in Materials and Methods. Although the staining of L22P-CDEFG by MAb 21-1 was hardly detectable, a few cells exhibited weak but significant cytoplasmic fluorescence, which was regarded as being faint (f in Fig. 3). Magnification, $\times 135$.

going conformational changes that lead to cell fusion. We have therefore concluded that there is a striking difference in the native (prefusion) conformation between nonfusogenic WR F protein and its fusogenic mutant, L22P. It should be stressed, however, that our present data do not exclude the possibility that the MAb epitopes may also be present in the postfusion conformation of L22P.

The epitopes for MAbs 6-7 and 21-1 in the WR F protein could be exposed by heating at 47°C as efficiently as could those in L22P (Table 2), indicating that at this temperature the structure of the WR F protein might be similar to that of L22P. Interestingly, in this context, Paterson et al. (39) have reported that the WR F protein can induce membrane fusion between erythrocytes and CV1 cells at 53°C when it is coexpressed with (uncleaved) influenza virus hemagglutinin in CV1 cells in the recombinant vaccinia virus-T7 expression system. Therefore, the structure of the WR F protein at 47°C may include a conformation that it adopts during the course of inducing cell fusion. However, in our plasmid expression system using HeLa cells, the WR F protein could not induce cell fusion by itself even when heated at 47 or 53°C (our unpublished data). There is a reasonable possibility that this discrepancy reflects the difference in sensitivity between our cell fusion assay and that (lipid mixing and content mixing assays) of Paterson et al. (39). Interestingly, the results obtained from immunoprecipitation analysis have demonstrated that MAbs 6-7 and 21-1 can precipitate the WR F protein as efficiently as they can immunoprecipitate L22P, indi-

cating that the MAb epitopes can also be exposed on the WR F protein by detergent solubilization as well as on L22P. Alternatively, the conformation of the detergent-solubilized F protein seems not to be identical to the native conformation.

Recently, it has been demonstrated that there is difference in conformation between uncleaved and cleaved SV5F protein as studied by immunoprecipitation and flow cytometric analyses (13). Although our immunoprecipitation analysis has indicated that MAb 6-7 reacts more efficiently with the cleaved form than with the uncleaved form (Fig. 1B), the difference seems less clear than the reported data (13). Furthermore, in the flow cytometric analysis, the MAb can react with the uncleaved form even better than with the cleaved form. Therefore, the discrepancy in the MAb 6-7 reactivity between our immunoprecipitation and flow cytometry analyses may reflect the difference in conformation between detergent-solubilized and native F proteins, as discussed above. Taking these results together, we conclude that MAb 6-7 cannot distinguish the reported difference found between cleaved and uncleaved forms of SV5F protein.

As indicated by the results of chimeric analysis, the epitopes for MAbs 6-7 and 21-1 are located within block D (the middle region of F1, which includes the HR3 domain) of L22P. In addition to block D, L22P-derived block A (the amino-terminal region of F2) is required to form the MAb 21-1 epitope. However, since block A does not serve as the epitope for MAb 21-1 by itself and since MAb 21-1 reacts only faintly with block

D unless it is combined with block A (Fig. 3), we cannot discriminate between the following two possibilities. (i) The MAb 21-1 epitope in L22P is composed solely of amino acids in block D but is somehow hidden by F2 when block A is replaced with that of SV41 F protein or the WR F protein. (ii) The MAb 21-1 epitope in L22P is composed mainly of amino acids in block D but a few in the block A are also used; a proper distance between these blocks forms the MAb 21-1 epitope. Since MAb 21-1 can recognize the WR F protein as well as L22P after heat denaturation, it seems unlikely that Pro-22 itself is a constituent of the MAb 21-1 epitope. Taken together, it can be hypothesized that Leu-22 in the WR F protein somehow directs a tight association between the F1 and F2 subunits. As a result, steric hindrance of block D by F2 may occur or the distance between blocks A and D may become inadequate for formation of the MAb 21-1 epitope. Our present data thus suggest that the putative F1-F2 interaction in the WR F protein involves the amino-terminal region of F2 and the middle region of F1 that includes the HR3 domain. Interestingly, a topological interrelationship between F1 (HR1 domain or cysteine-rich region) and F2 (middle region) of the Newcastle disease virus F protein has been suggested by studies on neutralization escape mutants (35, 48, 55) or on temperature-sensitive mutants and the revertants (59).

On the other hand, the poor reactivity of MAb 6-7 with the native WR F protein also seems to be due to its Leu-22 in the F2, since the MAb epitope (block D) is shared by L22P and the WR F protein. Presumably, in the case of the WR F protein, F2 somehow hinders the MAb 6-7 epitope (block D in F1), as we supposed above for the MAb 21-1 epitope.

The intervening sequence between the HR1 and HR2 domains is very long and is a characteristic of the paramyxovirus F protein (1). The F protein is predicted to undergo conformational changes during the fusion process: formation of the trimeric coiled-coil structure of HR1, insertion of the fusion peptide into the target membrane, and antiparallel association of the HR2 domain to the trimeric HR1 coiled coil, as illustrated by Baker et al. (1). For this purpose, the long intervening sequence should undergo complex and sequential conformational changes at right time and at right place. For most paramyxoviruses except for SV5 strain W3A, it has been assumed that HN undergoes a conformational change on binding to cellular receptor, which then triggers a conformational change of the F protein via an HN-F interaction (30). We hypothesize that the putative tight interaction between F2 and F1 stabilizes WR F1 and prevents it from undergoing conformational changes that lead to fusion until it is triggered by HN protein. This assumption is analogous to a model for human immunodeficiency virus gp41-mediated membrane fusion (8) in which the gp41 structure is stabilized by its interaction with gp120 in the native state. When gp120 binds to cell surface CD4 and a chemokine receptor, a conformational change occurs in gp120 that alters gp120-gp41 interactions, which then triggers gp41 to undergo its conformational changes that lead to fusion. For L22P, the putative interaction between F2 and F1 may be loose due to Pro-22, thus resulting in exposure or formation of the MAb 21-1 epitope. Moreover, the loose F1-F2 interaction may destabilize L22P, which thus easily undergoes conformational changes that lead to fusion by yet unidentified trigger(s). This view is consistent with the assump-

tion of Paterson et al. that Pro-22 somehow destabilizes the W3A F protein and facilitates the HN-independent fusion activity (39). Taking these results together, the destabilized structure of native L22P may represent an intermediate between the prefusion and postfusion conformations of a typical paramyxovirus F protein. This putative intermediate may well be formed transiently in the latter protein. Interestingly, another destabilizing amino acid, Pro-443, which is located immediately upstream of the HR2 domain has been identified in the WR F protein (and thus in L22P) (39).

We have recently demonstrated by chimeric analysis of L22P and the SV5 (strain T1) F protein that 132-Glu in the HR1 domain is also responsible for the HN-independent fusion activity of L22P (28). However, its role played in the HN-independent fusion activity is still unclear. On the other hand, mutational analysis of the Newcastle disease virus F protein has demonstrated that a mutant protein, whose Leu-289 in the HR3 domain is replaced with Ala, is able to mediate syncytium formation in the absence of HN (43). In this context, our observation that Ala-290 in the HR3 domain of L22P contributes to the HN-independent fusion activity to some extent (28) is interesting. It is unclear how those amino acids in the HR3 domain contribute to the fusing activity, although a study of Sendai virus F protein has indicated that the peptide representing the HR3 domain can self-assemble or can coassemble with the HR1 or HR2 peptides (19). Furthermore, the peptide representing the HR3 domain is known to inhibit Sendai virus-mediated hemolysis (18). However, the HR3 peptide of SV5 does not specifically interact with the HR1 peptide and is not considered a component in the final, most stable core of the F protein, the antiparallel trimeric coiled-coil structure (14). Since the HR3 peptide of SV5 is prone to aggregate in solution (14), the HR3 domain may participate in the stabilization of the oligomeric structure of the F protein in its native state, as supposed for Sendai virus (18). If this is the case, the putative tight interaction of the F1 middle region (including HR3 domain) with F2, which has been assumed for native WR F protein, may also contribute to this kind of stabilization.

ACKNOWLEDGMENTS

We acknowledge Satoru Ogawa for excellent technical assistance in confocal laser microscopy. We thank Yutaka Takebe for kindly providing the plasmid vectors pcDL-SR α 296 and pKan2. We are also grateful to Kiyoshi Tanabayashi and Akio Yamada for their generous gift of recombinant plasmid encoding MuV HN protein.

This work was supported by a Grant-in-Aid for Scientific Research (grant 12670280) from the Ministry of Education, Culture, Sports, Science and Technology, Japan.

REFERENCES

1. Baker, K. A., R. E. Dutch, R. A. Lamb, and T. S. Jardetzky. 1999. Structural basis for paramyxovirus-mediated membrane fusion. *Mol. Cell* 3:309-319.
2. Bousse, T., T. Takimoto, W. L. Gorman, T. Takahashi, and A. Portner. 1994. Regions on the hemagglutinin-neuraminidase proteins of human parainfluenza virus type-1 and Sendai virus important for membrane fusion. *Virology* 204:506-514.
3. Bullough, P. A., F. M. Hughson, J. J. Skehel, and D. C. Wiley. 1994. Structure of influenza haemagglutinin at the pH of membrane fusion. *Nature* 371:37-43.
4. Caffrey, M., M. Cai, J. Kaufman, S. J. Stahl, P. T. Wingfield, D. G. Covell, A. M. Gronenborn, and G. M. Clore. 1998. Three-dimensional solution structure of the 44 kDa ectodomain of SIV gp41. *EMBO J.* 17:4572-4584.
5. Calder, L. J., L. González-Reyes, B. García-Barreno, S. A. Wharton, J. J. Skehel, D. C. Wiley, and J. A. Melerio. 2000. Electron microscopy of the human respiratory syncytial virus fusion protein and complexes that it forms

- with monoclonal antibodies. *Virology* **271**:122–131.
6. **Chambers, P., C. R. Pringle, and A. J. Easton.** 1992. Sequence analysis of the gene encoding the fusion glycoprotein of pneumonia virus of mice suggests possible conserved secondary structure elements in paramyxovirus fusion glycoproteins. *J. Gen. Virol.* **73**:1717–1724.
 7. **Chan, D. C., D. Fass, J. M. Berger, and P. S. Kim.** 1997. Core structure of gp41 from the HIV envelope glycoprotein. *Cell* **89**:263–273.
 8. **Chan, D. C., and P. S. Kim.** 1997. HIV entry and its inhibition. *Cell* **93**:681–684.
 9. **Collins, P. L., R. M. Chanock, and K. McIntosh.** 1996. Parainfluenza viruses, p. 1205–1241. *In* B. N. Fields, D. M. Knipe, P. M. Howley, R. M. Chanock, J. L. Melnick, T. P. Monath, B. Roizman, and S. E. Straus (ed.), *Fields virology*, 3rd ed., vol. 1. Lippincott-Raven Publishers, Philadelphia, Pa.
 10. **Deng, R., A. M. Mirza, P. J. Mahon, and R. M. Iorio.** 1997. Functional chimeric HN glycoproteins derived from Newcastle disease virus and human parainfluenza virus-3. *Arch. Virol.* **13**(Suppl.):115–130.
 11. **Deng, R., Z. Wang, P. J. Mahon, M. Marinello, A. Mirza, and R. M. Iorio.** 1999. Mutations in the Newcastle disease virus hemagglutinin-neuraminidase protein that interfere with its ability to interact with the homologous F protein. *Virology* **253**:43–54.
 12. **Deng, R., Z. Wang, A. M. Mirza, and R. M. Iorio.** 1995. Localization of a domain on the paramyxovirus attachment protein required for the promotion of cellular fusion by its homologous fusion protein spike. *Virology* **209**:457–469.
 13. **Dutch, R. E., R. N. Hagglund, M. A. Nagel, R. G. Paterson, and R. A. Lamb.** 2001. Paramyxovirus fusion protein: a conformational change on cleavage activation. *Virology* **281**:138–150.
 14. **Dutch, R. E., G. P. Leser, and R. A. Lamb.** 1999. Paramyxovirus fusion protein: characterization of the core trimer, a rod-shaped complex with helices in anti-parallel orientation. *Virology* **254**:147–159.
 15. **Ebata, S. N., M.-J. Côté, C. Yong Kang, and K. Dimock.** 1991. The fusion and hemagglutinin-neuraminidase glycoproteins of human parainfluenza virus 3 are both required for fusion. *Virology* **183**:437–441.
 16. **Ebata, S. N., L. Prevec, F. L. Graham, and K. Dimock.** 1992. Function and immunogenicity of human parainfluenza virus 3 glycoproteins expressed by recombinant adenoviruses. *Virus Res.* **24**:21–33.
 17. **Gething, M.-J., J. M. White, and M. D. Waterfield.** 1978. Purification of the fusion protein of Sendai virus: analysis of the NH2-terminal sequence generated during precursor activation. *Proc. Natl. Acad. Sci. USA* **75**:2737–2740.
 18. **Ghosh, J. K., M. Ovdia, and Y. Shai.** 1997. A leucine zipper motif in the ectodomain of Sendai virus fusion protein assembles in solution and in membranes and specifically binds biologically-active peptides and the virus. *Biochemistry* **36**:15451–15462.
 19. **Ghosh, J. K., S. G. Peisajovich, M. Ovdia, and Y. Shai.** 1998. Structure-function study of a heptad repeat positioned near the transmembrane domain of Sendai virus fusion protein which blocks virus-cell fusion. *J. Biol. Chem.* **273**:27182–27190.
 20. **Graham, F. L., and A. J. van der Eb.** 1973. A new technique for the assay of infectivity of human adenovirus 5 DNA. *Virology* **52**:456–467.
 21. **Heminway, B. R., Y. Yu, and M. S. Galinski.** 1994. Paramyxovirus mediated cell fusion requires co-expression of both the fusion and hemagglutinin-neuraminidase glycoproteins. *Virus Res.* **31**:1–16.
 22. **Homma, M., and M. Ohuchi.** 1973. Trypsin action on the growth of Sendai virus in tissue culture cells. III. Structural differences of Sendai virus grown in eggs and tissue culture cells. *J. Virol.* **12**:1457–1465.
 23. **Homma, M., and S. Tamagawa.** 1973. Restoration of the fusion activity of L cell-borne Sendai virus by trypsin. *J. Gen. Virol.* **19**:423–426.
 24. **Horvath, C. M., R. G. Paterson, M. A. Shaughnessy, R. Wood, and R. A. Lamb.** 1992. Biological activity of paramyxovirus fusion proteins: factors influencing formation of syncytia. *J. Virol.* **66**:4564–4569.
 25. **Hsu, M.-C., A. Scheid, and P. W. Choppin.** 1981. Activation of the Sendai virus fusion protein (F) involved a conformational change with exposure of a new hydrophobic region. *J. Biol. Chem.* **256**:3557–3565.
 26. **Hu, X., R. Ray, and R. W. Compans.** 1992. Functional interactions between the fusion protein and hemagglutinin-neuraminidase of human parainfluenza viruses. *J. Virol.* **66**:1528–1534.
 27. **Ito, M., M. Nishio, M. Kawano, S. Kusagawa, H. Komada, Y. Ito, and M. Tsurudome.** 1997. Role of a single amino acid at the amino terminus of the simian virus 5 F2 subunit in syncytium formation. *J. Virol.* **71**:9855–9858.
 28. **Ito, M., M. Nishio, H. Komada, Y. Ito, and M. Tsurudome.** 2000. An amino acid in the heptad repeat 1 domain is important for the haemagglutinin-neuraminidase-independent fusing activity of simian virus 5 fusion protein. *J. Gen. Virol.* **81**:719–727.
 29. **Kohama, T., W. Garten, and H.-D. Klenk.** 1981. Changes in conformation and charge paralleling proteolytic activation of Newcastle disease virus glycoproteins. *Virology* **111**:364–376.
 30. **Lamb, R. A.** 1993. Paramyxovirus fusion: a hypothesis for changes. *Virology* **197**:1–11.
 31. **Lamb, R. A., and D. Kolakofsky.** 1996. Paramyxoviridae: the viruses and their replication, p. 1177–1204. *In* B. N. Fields, D. M. Knipe, P. M. Howley, R. M. Chanock, J. L. Melnick, T. P. Monath, B. Roizman, and S. E. Straus (ed.), *Fields virology*, 3rd ed., vol. 1, Lippincott-Raven Publishers, Philadelphia, Pa.
 32. **Leser, G. P., K. J. Ector, and R. A. Lamb.** 1996. The paramyxovirus simian virus 5 hemagglutinin-neuraminidase glycoprotein, but not the fusion glycoprotein, is internalized via coated pits and enters the endocytic pathway. *Mol. Biol. Cell* **7**:155–172.
 33. **Matthews, J. M., T. F. Young, S. P. Tucker, and J. P. Mackay.** 2000. The core of the respiratory syncytial virus fusion protein is a trimeric coiled coil. *J. Virol.* **74**:5911–5920.
 34. **Morrison, T., C. McQuain, and L. McGinnes.** 1991. Complementation between avirulent Newcastle disease virus and a fusion protein gene expressed from a retrovirus vector: requirements for membrane fusion. *J. Virol.* **65**:813–822.
 35. **Neyt, C., J. Geliebter, M. Slaoui, D. Morales, G. Meulemans, and A. Burny.** 1989. Mutations located on both F1 and F2 subunits of the Newcastle disease virus fusion protein confer resistance to neutralization with monoclonal antibodies. *J. Virol.* **63**:952–954.
 36. **Nishio, M., M. Tsurudome, H. Komada, M. Kawano, N. Tabata, H. Matsumura, N. Ikemura, N. Watanabe, and Y. Ito.** 1994. Fusion properties of cells constitutively expressing human parainfluenza virus type 4A haemagglutinin-neuraminidase and fusion glycoproteins. *J. Gen. Virol.* **75**:3517–3523.
 37. **Novick, S. L., and D. Hoekstra.** 1988. Membrane penetration of Sendai virus glycoproteins during the early stages of fusion with liposomes as determined by hydrophobic photoaffinity labeling. *Proc. Natl. Acad. Sci. USA* **85**:7433–7437.
 38. **Paterson, R. G., S. W. Hiebert, and R. A. Lamb.** 1985. Expression at the cell surface of biologically active fusion and hemagglutinin/neuraminidase proteins of the paramyxovirus simian virus 5 from cloned cDNA. *Proc. Natl. Acad. Sci. USA* **82**:7520–7524.
 39. **Paterson, R. G., C. J. Russell, and R. A. Lamb.** 2000. Fusion protein of the paramyxovirus SV5: destabilizing and stabilizing mutants of fusion activation. *Virology* **270**:17–30.
 40. **Pringle, C. R.** 1999. Virus taxonomy—1999. The universal system of virus taxonomy, updated to include the new proposals ratified by the international committee on taxonomy of viruses during 1998. *Arch. Virol.* **144**:421–429.
 41. **Sakai, Y., and H. Shibuta.** 1989. Syncytium formation by recombinant vaccinia viruses carrying bovine parainfluenza 3 virus envelope protein genes. *J. Virol.* **63**:3661–3668.
 42. **Scheid, A., and P. W. Choppin.** 1974. Identification and biological activities of paramyxovirus glycoproteins. Activation of cell fusion, hemolysis, and infectivity by proteolytic cleavage of an inactive precursor protein of Sendai virus. *Virology* **57**:475–490.
 43. **Sergel, T. A., L. W. McGinnes, and T. G. Morrison.** 2000. A single amino acid change in the Newcastle disease virus fusion protein alters the requirement for HN protein in fusion. *J. Virol.* **74**:5101–5107.
 44. **Stone-Hulslander, J., and T. G. Morrison.** 1997. Detection of an interaction between the HN and F proteins in Newcastle disease virus-infected cells. *J. Virol.* **71**:6287–6295.
 45. **Tabata, N., M. Ito, K. Shimokata, S. Suga, S. Ohgimoto, M. Tsurudome, M. Kawano, H. Matsumura, H. Komada, M. Nishio, and Y. Ito.** 1994. Expression of fusion regulatory proteins (FRPs) on human peripheral blood lymphocytes. Induction of homotypic cell aggregation and formation of multinucleated giant cells by anti-FRP-1 monoclonal antibody. *J. Immunol.* **153**:3256–3266.
 46. **Tanabayashi, K., and R. W. Compans.** 1996. Functional interaction of paramyxovirus glycoproteins: identification of a domain in Sendai virus HN which promotes cell fusion. *J. Virol.* **70**:6112–6118.
 47. **Tanabayashi, K., K. Takeuchi, K. Okazaki, M. Hishiyama, and A. Yamada.** 1992. Expression of mumps virus glycoproteins in mammalian cells from cloned cDNAs: both F and HN proteins are required for cell fusion. *Virology* **187**:801–804.
 48. **Toyoda, T., B. Gotoh, T. Sakaguchi, H. Kida, and Y. Nagai.** 1988. Identification of amino acids relevant to three antigenic determinants on the fusion protein of Newcastle disease virus that are involved in fusion inhibition and neutralization. *J. Virol.* **62**:4427–4430.
 49. **Tsurudome, M., H. Bando, M. Nishio, Y. Iwamoto, M. Kawano, K. Kondo, H. Komada, and Y. Ito.** 1990. Antigenic and structural properties of a paramyxovirus simian virus 41 (SV41) reveal a close relationship with human parainfluenza type 2 virus. *Virology* **179**:738–748.
 50. **Tsurudome, M., M. Ito, M. Nishio, M. Kawano, K. Okamoto, S. Kusagawa, H. Komada, and Y. Ito.** 1998. Identification of regions on the fusion protein of human parainfluenza type 2 virus which are required for haemagglutinin-neuraminidase proteins to promote cell fusion. *J. Gen. Virol.* **79**:279–289.
 51. **Tsurudome, M., M. Kawano, T. Yuasa, N. Tabata, M. Nishio, H. Komada, and Y. Ito.** 1995. Identification of regions on the hemagglutinin-neuraminidase protein of human parainfluenza virus type 2 important for promoting cell fusion. *Virology* **213**:190–203.
 52. **Tsurudome, M., M. Nishio, H. Komada, H. Bando, and Y. Ito.** 1989. Extensive antigenic diversity among human parainfluenza type 2 virus isolates and immunological relationships among paramyxoviruses revealed by monoclonal antibodies. *Virology* **171**:38–48.

53. **Tsurudome, M., A. Yamada, M. Hishiyama, and Y. Ito.** 1986. Monoclonal antibodies against the glycoproteins of mumps virus: fusion inhibition by anti-HN monoclonal antibody. *J. Gen. Virol.* **67**:2259–2265.
54. **Umino, Y., T. Kohama, T. A. Sato, A. Sugiura, H.-D. Klenk, and R. Rott.** 1990. Monoclonal antibodies to three structural proteins of Newcastle disease virus: biological characterization with particular reference to the conformational change of envelope glycoproteins associated with proteolytic cleavage. *J. Gen. Virol.* **71**:1189–1197.
55. **Wang, C., G. Raghu, T. Morrison, and M. E. Peeples.** 1992. Intracellular processing of the paramyxovirus F protein: critical role in the predicted amphipathic alpha helix adjacent to the fusion domain. *J. Virol.* **66**:4161–4169.
56. **Weissenhorn, W., A. Carfi, K.-H. Lee, J. J. Skehel, and D. C. Wiley.** 1998. Crystal structure of the Ebola virus membrane fusion subunit, GP2, from the envelope glycoprotein ectodomain. *Mol. Cell* **2**:605–616.
57. **Weissenhorn, W., A. Dessen, S. C. Harrison, J. J. Skehel, and D. C. Wiley.** 1997. Atomic structure of the ectodomain from HIV-1 gp41. *Nature* **347**:426–430.
58. **Yao, Q., X. Hu, and R. W. Compans.** 1997. Association of the parainfluenza virus fusion and hemagglutinin-neuraminidase glycoproteins on cell surfaces. *J. Virol.* **71**:650–656.
59. **Yusoff, K., M. Nesbit, H. McCarthy, G. Meulemans, D. J. Alexander, M. S. Collins, P. T. Emmerson, and A. C. R. Samson.** 1989. Location of neutralizing epitopes on the fusion protein of Newcastle disease virus strain Beaudette C. *J. Gen. Virol.* **70**:3105–3109.
60. **Zhao, X., M. Singh, V. N. Malashkevich, and P. S. Kim.** 2000. Structural characterization of the human respiratory syncytial virus fusion protein core. *Proc. Natl. Acad. Sci. USA* **97**:14172–14177.